CHAPTER – 4

Synthesis and Characterization of Al - substituted Magnetite Nanoparticles

4.1 Introduction

In the last chapter, it has been discussed that Zr or Hf-substituted magnetite nanoparticles show that the T_S between 42 - 46 °C can be achieved during magnetic hyperthermia. This happened despite of their high saturation magnetization (M_S) values, high T_C values (>302 °C) and high concentration of MNPs (40 mg/mL). However, the salts of Zr or Hf are quite costly. Thus, a cheaper element i.e. Al was selected to explore its effect on the T_S values. Hence, trivalent non-magnetic cations substituted magnetite ($Al_xFe_{3-x}O_4$, $0.01 \leq x \leq 1$) samples were synthesized by microwave refluxing technique. The synthesis protocol for these samples was identical to that Zr or Hf substituted samples which have been discussed in Chapter-2. Structural, microstructural and magnetic properties characterizations were carried out to understand the effect of Al^{3+}-ion substitutions. MHT experiments were performed using ferrofluids of Al^{3+}-substituted magnetite nanoparticles to determine the T_S values at various fields. Simultaneously, the specific absorption rate (SAR, W/g) were estimated to determine the heating ability for the samples.

4.2 Al substituted magnetite nanoparticles

4.2.1 XRD analysis

XRD patterns of $Al_xFe_{3-x}O_4$ ($0.01 \leq x \leq 1$) samples are shown in Fig. 4.2.1(a). The peaks for all the samples were similar to that of pure magnetite having space group Fd3m. There were no other peaks which suggest about the absence of any impurity phase in the materials. Thus, within the limit of XRD measurement, the samples were essentially single phase and Al^{3+} could substitute Fe-ions.

Further, the variations in the lattice parameter of magnetite as a function of Al concentrations are given in Fig. 4.2.1 (b). The lattice parameter was found to be increasing slightly with increased Al^{3+}-ions concentration ($x \leq 0.01$). Nevertheless, the lattice parameter found to be decreasing continuously for $x \geq 0.1$. The ionic radii of Al^{3+}, Fe^{2+} and Fe^{3+} ions at tetrahedral sites are 0.53, 0.77 and 0.63 Å and at octahedral sites are 0.68, 0.92 and 0.79 Å respectively. Thus, the substitution of Al^{3+} ions in Fe_3O_4 may take place at any of the voids. The earlier reports on Al-substituted iron oxides suggest that Al initially replace Fe-ions at the octahedral voids up to a certain concentration (around $x = 0.1$ in the present case) and then to the tetrahedral voids. The smaller ionic radii of Al^{3+} ions could be the reasons for reduced lattice parameters at higher concentration.

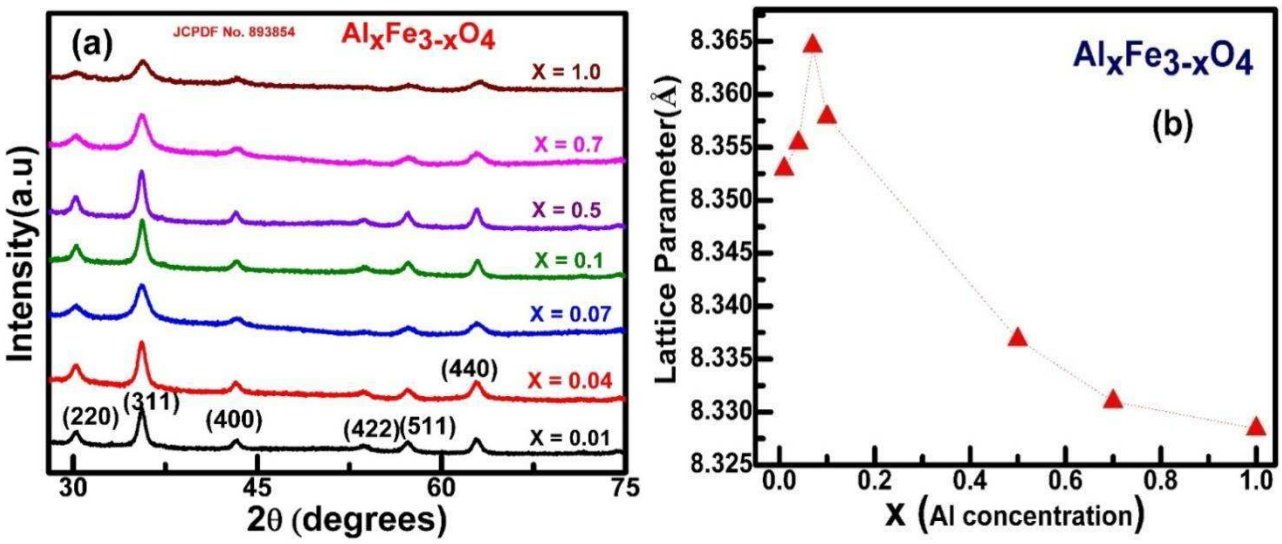

Fig.4.2.1: (a) XRD patterns for $Al_xFe_{3-x}O_4$ (x = 0.01, 0.07, 0.1, 0.5, 0.7 and 1.0) samples and (b) lattice parameter variation with Al content.

The average crystallite size for $Al_xFe_{3-x}O_4$ ($0.01 \leq x \leq 1$) samples was calculated using Scherrer's formula. The average crystallite size was found to be in the range of 3 to 5 nm.

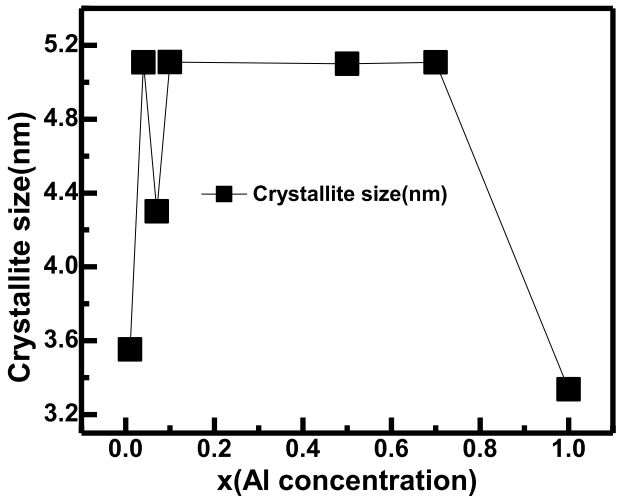

Fig.4.2.2: The variation of crystallite size with Al content for $Al_xFe_{3-x}O_4$ (x = 0.01, 0.07, 0.1, 0.5, 0.7 and 1.0) samples.

4.2.2 TEM analysis

The bright field TEM micrographs along with SAD patterns for $Al_{0.07}Fe_{2.93}O_4$ and $Al_{0.7}Fe_{2.3}O_4$ samples are shown in Figs. 4.2.3 (a) and (c) respectively. The morphology of the as prepared samples was almost spherical in shape. The particles size was found to be in the range 4- 25 nm. Selected area diffraction patterns as shown in the insets of Figs. 4.2.3 (a) and (c) also confirmed their FCC structure similar to magnetite.

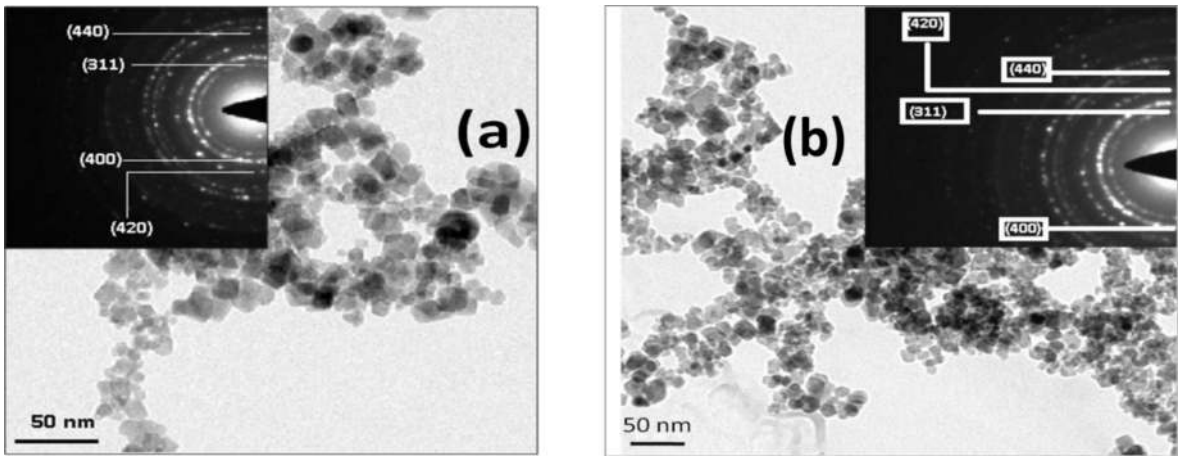

Fig.4.2.3: TEM micrographs for (a) $Al_{0.07}Fe_{2.93}O_4$ and (b) $Al_{0.7}Fe_{2.3}O_4$ samples. (Insets show corresponding SAD patterns).

4.2.3 XPS analysis

The X-ray photoelectron spectra for Al2p, Fe2p and O1s of the samples with x = 0.7 have been shown in Fig.4.2.4. The peaks of Fe $2p_{3/2}$ are greater than peaks of Fe $2p_{1/2}$ due to spin-orbit coupling. The deconvolution of the Fe 2p core level spectrum contains two peaks Fe^{3+} $2p_{3/2}$ and $2p_{1/2}$. The major peaks values were 712.69 eV and 724.49 eV respectively[72]. The satellite peaks of Fe $2p_{3/2}$ and Fe $2p_{1/2}$ were 711.07 eV and 720.09 eV. In addition, the peaks of Fe^{2+} $2p_{3/2}$ and $2p_{1/2}$ were observed at binding energies of 712 eV and 723.8 eV respectively. In spite of, the peaks of Al 2p(Al-oxide), Al 2p (metal) and Alumina at binding energies of 74.5 eV, 72.9 eV and 74.0 eV have been observed for Al 2p[73]. These suggest the presence of Al as Al^{3+} ion.

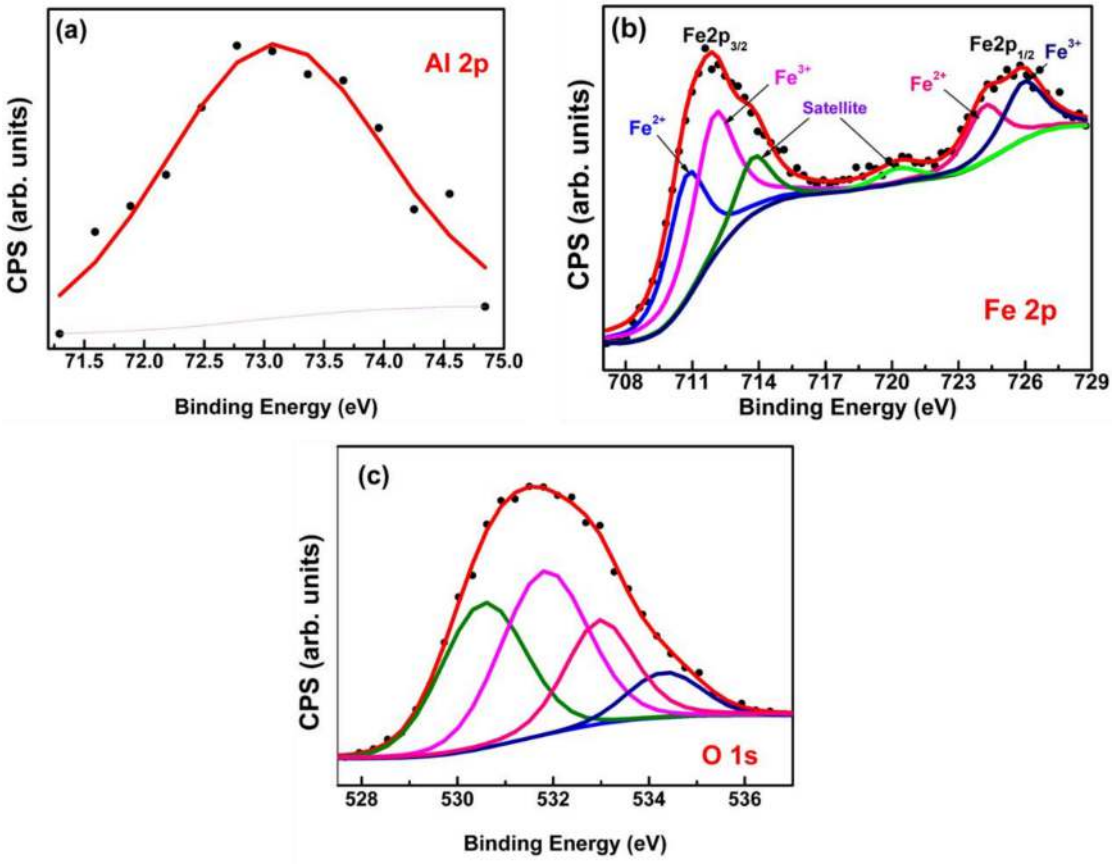

Fig. 4.2.4: XPS spectra of $Al_{0.7}Fe_{2.3}O_4$ sample (a) Al 2p (b) Fe 2p and(c) O1s core level.

4.2.4 Magnetic measurement analysis

The magnetization values for as prepared Al-substituted magnetite samples (x = 0.01, 0.04, 0.07, 0.1, 0.7, 1.0) were taken at ambient temperature and up to ±2 T field. The magnetizations vs. field curves are shown in Fig.4.2.5 (a). The variations in the M_S, M_r, and H_C values with respect to x are given in Fig.4.2.5 (b). The continuous decrement in the M_S values with increased Al^{3+} ions suggests that initially, Al^{3+}-ions might have occupied the octahedral sites of magnetite. However, at higher doping of Al^{3+} might have got distributed to both the voids of magnetite. The values of M_r and H_c for the samples were found to be very less which could be due to the presence of both ferrimagnetic and superparamagnetic component (Fig. 4.2.5 b). Such behaviour is obvious as the samples had particles of size in the range of 4 - 25 nm.

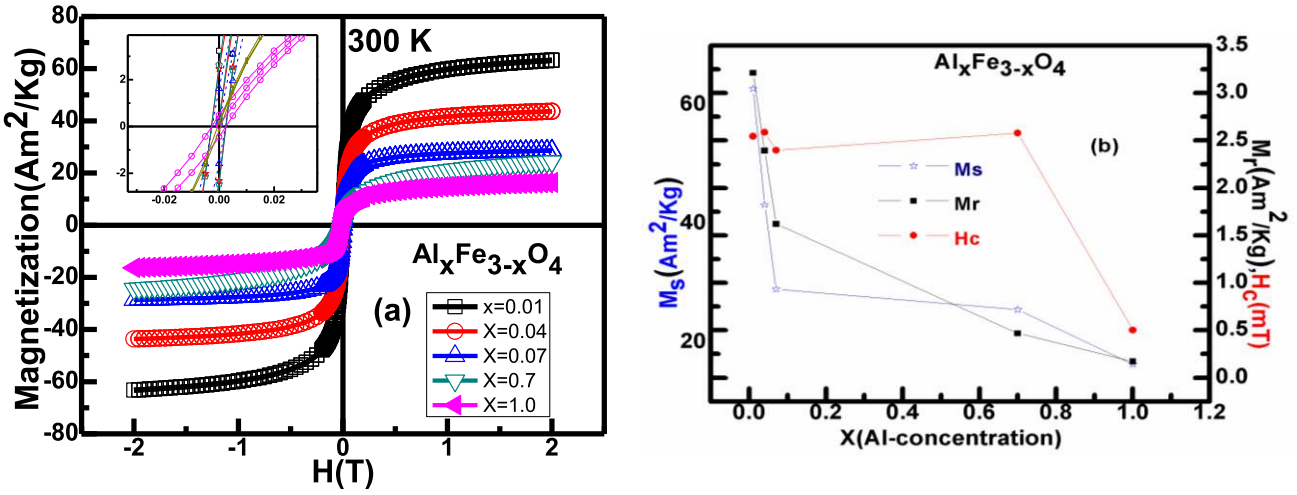

Fig. 4.2.5: (a) Magnetization vs. magnetic field curves at 300 K and ±2.0 T and (b) variation of M_S, M_r and H_C values for $Al_xFe_{3-x}O_4$ ($0.01 \leq x \leq 1.0$) samples.

4.2.5 Induction heating analysis

The heating ability for the ferrofluids prepared using MNPs of $Al_xFe_{3-x}O_4$ ($0.01 \leq x \leq 1$) was estimated at different combinations of field and frequency of AC magnetic fields. The procedure for preparation of the ferrofluids is discussed in chapter-2. A typical temperature vs. time curves for the samples at a field of amplitude of 9 mT and a frequency of 640 kHz are shown in figure 4.2.6 (a). The samples display continuous rise in the temperature beyond 60 °C for x = 0.04, 0.07 and 0.1 samples. In contrast, the samples x = 0.01, 0.5, 0.7 and 1.0 have shown stabilization of temperature (T_S) around 46, 31, 36 and 43 °C (Fig. 4.2.6 a). It has to be emphasized here that the sample with x = 0.01 had highest M_S value but has displayed stability of temperature but the sample with x = 1.0 has shown continuous rise. This behaviour was similar to that of the tetravalent ions doped magnetite, which is discussed in the chapter -3. It has also been observed that such behaviour was even independent of Curie temperature (T_C). The T_C values for these substituted magnetite were above 300 °C [18, 56–59].

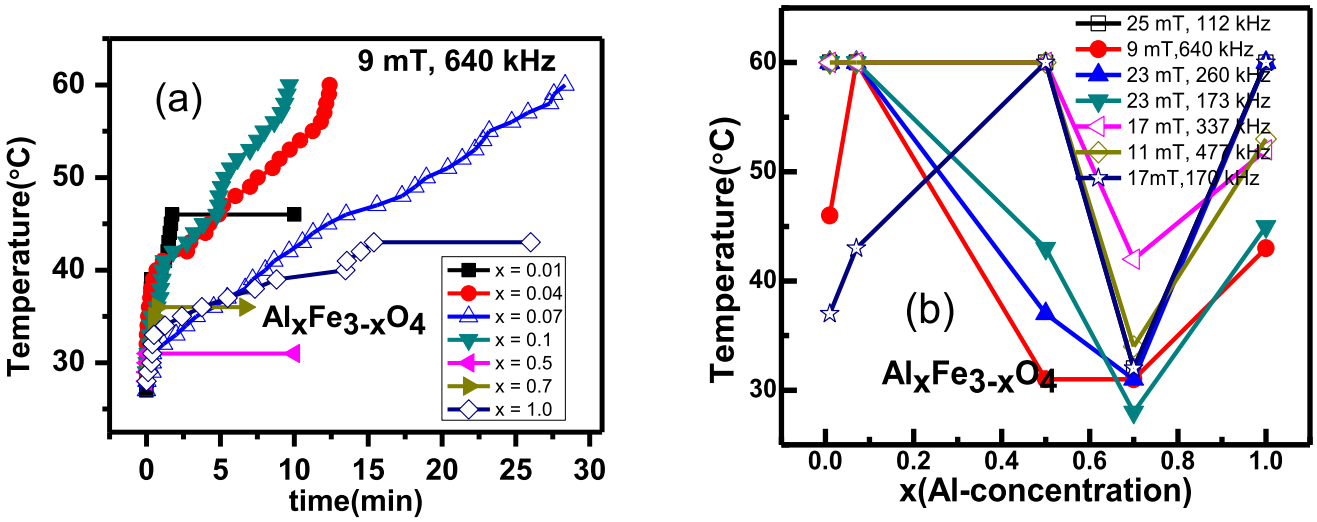

Fig. 4.2.6: (a) Temperature vs. time curves at a field of amplitude of 9 mT and a frequency of 640 kHz and (b) Temperature obtained during magnetic hyperthermia vs. Al-concentration curves at different fields and frequencies for $Al_xFe_{3-x}O_4$ ($0.01 \leq x \leq 1.0$) samples.

Similar experiments were carried out for the samples at various combinations of amplitude and frequency of external magnetic fields. The temperature reached during magnetic hyperthermia experiments are shown in Fig. 4.2.6 (b). The temperature observed near 60 °C suggests that the samples had shown continuous rise in the temperature in the presence of external magnetic fields. Nevertheless, at other fields, the samples have shown different T_S values which were similar to that of tetravalent ions doped magnetite Fig. 4.2.6 (b) (Chapter-3). This T_S values were found to be independent of magnetization value for the samples. The precise reasons for stabilization of temperature for the substituted magnetite samples during magnetic hyperthermia are not well understood and it needs further investigations.

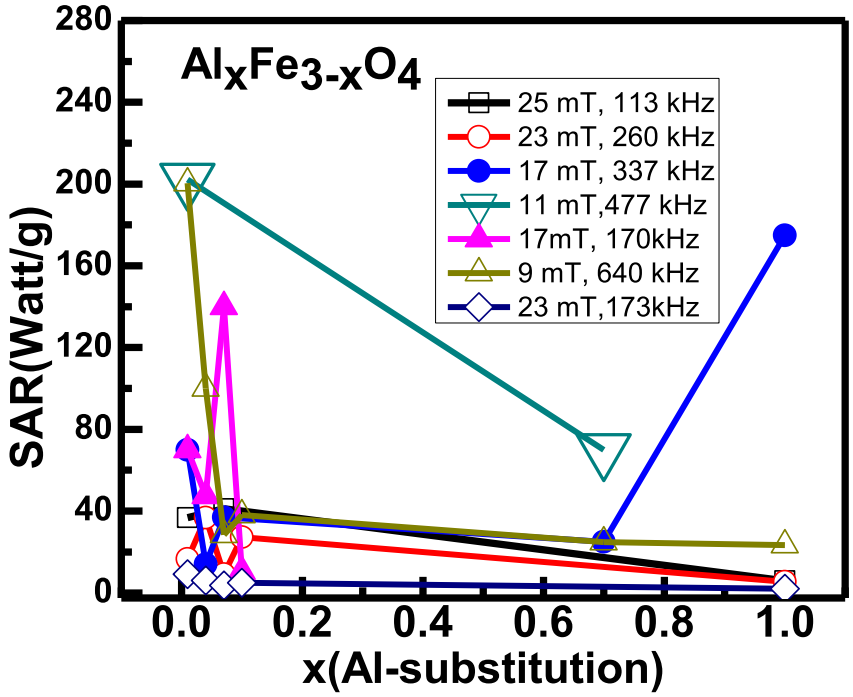

Fig. 4.2.7: The SAR values vs. Al substitution of $Al_xFe_{3-x}O_4$ ($0.01 \leq x \leq 1.0$) samples at different frequencies and fields.

The SAR values for $Al_xFe_{3-x}O_4$ based ferrofluids at various magnetic fields were determined using formula (given in chapter 2). The SAR (W/g) values of ferrofluids were completely dependent on the applied AC magnetic fields (Fig. 4.2.7). The calculated values of SAR might be different in the present case from the tetravalent substituted samples as well as some of the earlier reports in literature [18, 47, 56–59]. This may be due to the fact that SAR value rely on many aspects as properties (physiochemical) of carrier fluid, materials being used for coating, frequency and amplitude of external magnetic field, dispensability of MNPs [42, 52, 71, 72].

4.3 Conclusions

$Al_xFe_{3-x}O_4$ ($0.01 \leq x \leq 1$) samples were synthesized successfully by simple but effective one step microwave refluxing technique. Single phase were observed for all the concentration. There were continuous decrement in the lattice parameters after $x = 0.1$ for Al^{3+}substitution in Fe_3O_4 samples. Ferrimagnetic and superparamagnetic components were observed together in the sample due to particle of different sizes which was confirmed through hysteresis loops. The stabilizations of temperature at different fields were observed during MHT. Such ferrofluids may be extensively used for controlled MHT.